KECK Geology Consortium
Learning Science Through Research
Published by the Keck Geology Consortium
Short Contributions
Keck Geology Consortium
Volume 33
May 2020
doi: 10.18277/AKRSG.2020.33.08

CLIMATIC AND PALEOENVIRONMENTAL CHANGES ASSOCIATED WITH THE EVOLUTION OF *CORYPHODON* THROUGH PALEOGENE HYPERTHERMAL EVENTS, BIGHORN BASIN, WYOMING

ISAAC SAGEMAN, Northwestern University
Research Advisor: Matthew Hurtgen

INTRODUCTION

About 56 million years ago, during the Paleogene period, there was a massive global warming event termed the Paleocene-Eocene Thermal Maximum (PETM). This event featured a worldwide temperature increase of 5–8˚C, followed by a long-term warming trend that culminated with the Early Eocene Climatic Optimum (Zachos et al., 2008). This trend was emphasized by hyperthermal events similar, but smaller, to the PETM during the early Eocene (Abels et al., 2015). Climate changes drastically affect the resources available to animals, impacting their geographic ranges, growth rates, and reproductive behaviors (Barnosky et al., 2017). Some mammals experienced rapid dwarfing in response to the PETM and other hyperthermals (Gingerich, 2003; Secord et al., 2012; D'Ambrosia et al., 2017). This dwarfism is hypothesized to result from slower growth rates stemming from lower nutrition levels in plant resources (Gingerich, 2003); change in growth duration could also be a factor (Palkovacs, 2003).

To evaluate changes in body size in the Paleogene mammal *Coryphodon* during Paleogene climate change events, a precise chronostratigraphic framework of each site is necessary. This study seeks to provide such a framework by developing a bulk organic carbon isotope record for more than 20 *Coryphodon* localities from Late Paleocene strata in the Bighorn Basin of Northern Wyoming (Fig. 1A and B). Whereas the lithostratigraphic context of each site is described elsewhere, here I present geochemical analysis of each site in order to test for evidence of the PETM carbon isotope signature.

GEOLOGIC BACKGROUND

This study focuses on a bulk organic carbon isotope record from the Fort Union and Willwood Formations in the Bighorn Basin, Wyoming. The goal of this project is to provide a chronostratigraphic framework

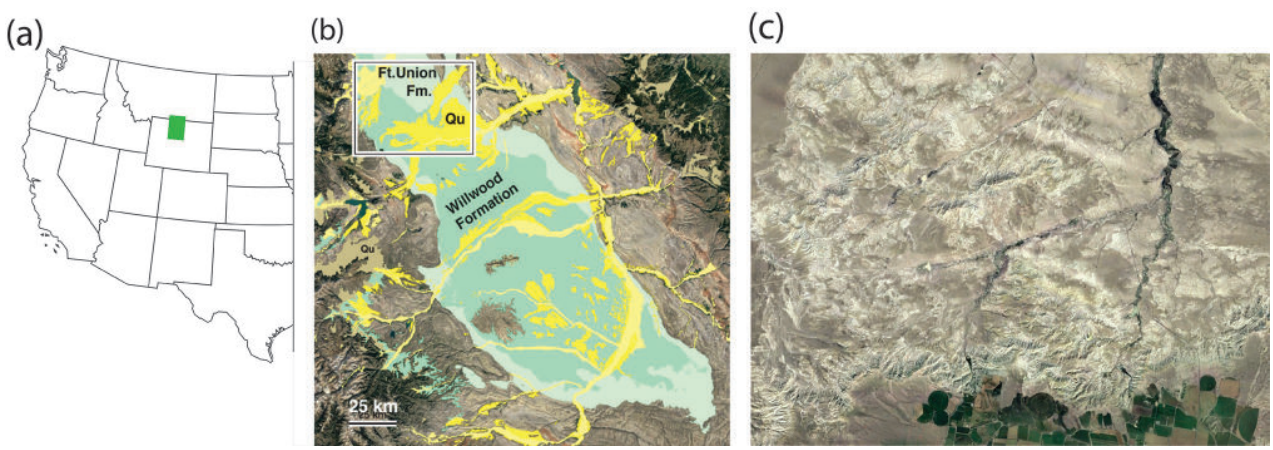

Figure 1. Overview of A) field area within the U.S., B) detail view of formations present in the broader study area, and C) the field area where samples were collected.

for *Coryphodon* samples collected from the Fort Union and Willwood Formations. The PETM is characterized by a prominent negative excursion in the $\delta^{13}C$ of organic matter and carbonate within the Willwood Formation of the Bighorn Basin (Baczynski et al., 2013). Analysis of $\delta^{13}C_{carb}$ in bulk samples of the Fort Union and Willwood Formations captures the isotopic mass balance of all carbonate contributions to the sample, which, based on the studies of Baczynski et al. (2013), could include pedogenic, biogenic, authigenic, and diagenetic carbonate.

METHODS

Fifteen stratigraphic sections containing a *Coryphodon*-bearing layer were measured in the northern Bighorn Basin (Fig. 1C; Fig. 2). Each section was trenched with hand tools and measured using a Jacob's staff while details of the lithofacies were recorded (grain size, soil color, bed contacts/thickness, sedimentary structures, soil mottling, presence of carbonate nodules, bioturbation, shells, fossil layers). Stratigraphic columns were created using Adobe Illustrator. Format and lithology can be seen in the right-hand column of Figure 3. The estimated stratigraphic order of these sections was determined using elevation and location coordinates measured with handheld GPS.

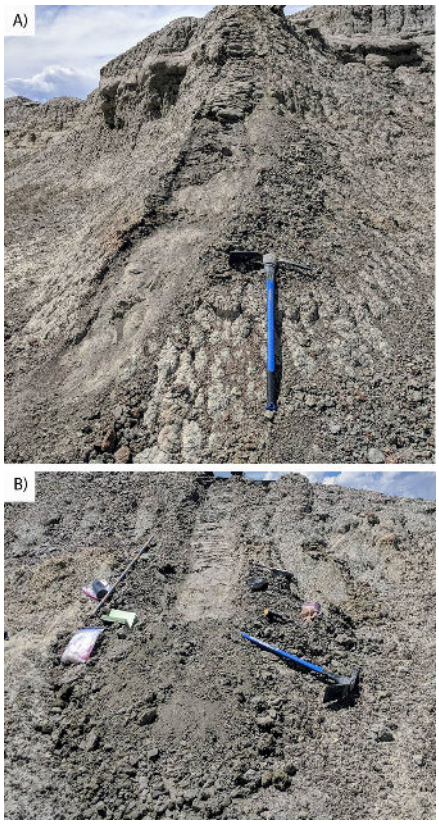

Figure 2. Field photographs of two stratigraphic sections, A) example in Fort Union Formation, and B) example in Willwood Formation.

A total of 93 fist-sized samples were taken at the base of each bed characterized by a different lithology. The samples were prepared for isotopic analysis by using an 8530 Shatterbox for rock crushing. Samples of 2–150 grams were placed into tungsten carbide cylinders with a puck. Three cylinders at a time were placed into the Shatterbox and run for 3 minutes until the sediment was reduced to a fine powder. After the tungsten carbide containers were clear of sample, they were thoroughly washed with DI water and dried using a compressed air stream before being placed into a desiccator for further drying.

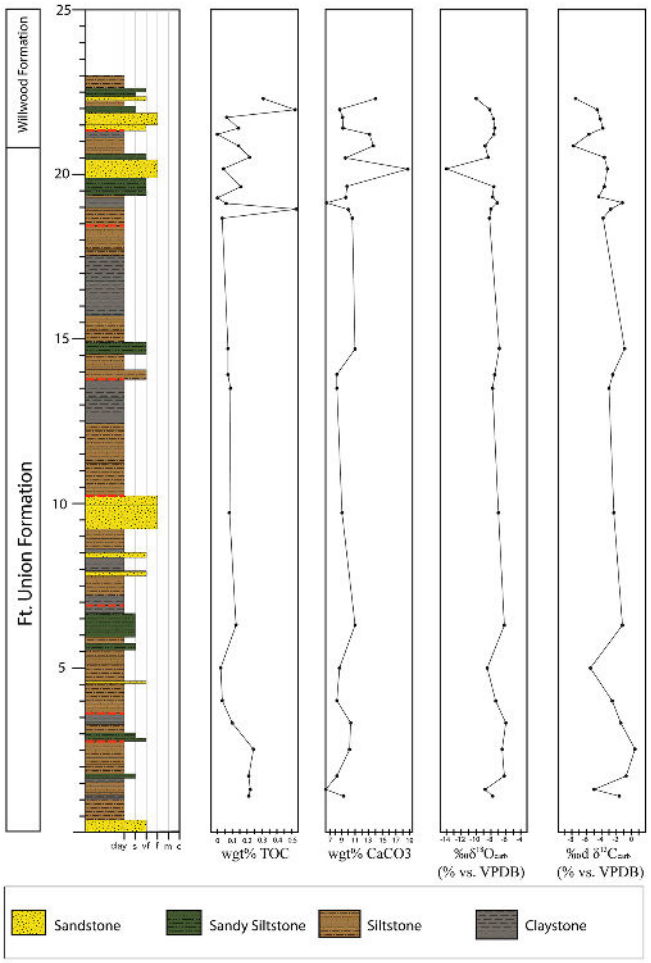

Figure 3. Change in wgt. % Total Organic Carbon (TOC), wgt. % Calcium Carbonate (CaCO3), wgt. ‰ δ13Ccarb, and wgt. ‰ δ18Ocarb up-section. Isotope data is correlated with specific samples from sections TC-01, MD-02, SH-07, KS-04, KS-01, ER-04, MD-19, and IS-07. Red dashed lines signify breaks between each individual stratigraphic column.

Coulometric analysis on a UIC Carbon Coulometer was performed in two steps 1) inorganic carbon assessment using acidification and 2) a total carbon assessment using combustion. The respective inorganic carbon and total carbon phases were converted to CO_2, and the amount of CO_2 evolved was measured coulometrically to yield wgt.% Total Inorganic Carbon (TIC) and wgt. % Total Carbon (TC) values; total organic carbon was determined by difference (TC-TIC), and wgt. % $CaCO_3$ was calculated from stoichiometry (TIC x 8.333). This procedure was done with an automated carbon dioxide coulometric titrator model 5030 following Engleman et al. (1985) for both oven and acid components.

Before weighing out samples for acid or oven analysis, all sample-carrying boats were either acidified or ignited to deplete any leftover material to avoid contamination. Blanks, carrying no sample, were run 3 times for later calculation purposes. Standards of 5.0 mg, 10 mg, 15 mg, 20 mg, and 25 mg ± 1.0 were weighed out using a Sartorius CPA2P Microbalance and ran before any samples in order to make sure the machines were performing correctly. The standards contain 12% $CaCO_3$ and generally the coulometer yields results for standards within 1%, indicating analytical uncertainty. Acid coulometry serves to determine inorganic carbon content of samples through the submersion of samples into 2 N perchloric acid for 5 minutes at a time. Oven coulometry yields the total carbon content of a sample through ignition of sample powders at 720˚C for 7 minutes inside the oven unit. The detection range for the instrument ranges from 0.01µg to 100 mg carbon. Both oven and acid results were recorded for each sample, along with their weights. I employed an external flow rate meter to correct for an inconsistency in flow rate within the oven's gas outlet.

I was able to perform measurements of $\delta^{13}C_{carb}$ by selecting samples with sufficient $CaCO_3$ based on carbon coulometry result;, 25 samples with $CaCO_3$ values of at least 8 wgt.% were selected for analysis. 400 ± 10 µg of each viable sample were weighed out using a Sartorius CPA2P Microbalance, transferred to Gasbench vials with pressure-sealed caps and measured on a Thermo Delta V plus.

RESULTS

Field Observations

The measured stratigraphic sections consisted of interbedded thin, diagenetically altered mud and claystone units as well as thin-bedded, light colored fluvial sandstones and conglomerates. The sandstone beds tended to be more massive and ranged from silty, very fine, to fine-grained. The diagenetically altered strata were mainly paleosol starting in the Fort Union Formation and continuing up through the Willwood Formation. These rhythmically alternating units are clearly visible in outcrop, as well as in the coulometry data described below.

Coulometry

Carbon coulometry resulted in $CaCO_3$ and TOC data that were useful for interpretation of facies changes, and guided the selection of samples for isotopic analysis. The data are illustrated in Figure 4 Values of wgt. % TC vary in a cyclic pattern going up-section, having an average value of 0.58% until the MD-19 section (Fig. 3 and 4) is reached, at which point the average increases to 1.48%. This change is additionally indicated in the other datasets, as the average wgt. % $CaCO_3$ raises from 3.82 up to 11.37%. The wgt. % TOC data shows an average value of 0.12% across all sections, but has 5 data points significantly higher than the others.

Gas Bench

The 25 samples with $CaCO_3$ values between 0 and 20% (± 2%) were measured on the Gasbench, producing $\delta^{13}C_{carb}$ and $\delta^{18}O_{carb}$ data. The samples ran well within precision on standards of s-$\delta^{13}C$ = 0.1 ‰ and s-δ18O = 0.15‰; average values for the data set were -3.3% for $\delta^{13}C_{carb}$ and -7.9% for $\delta^{18}O_{carb}$. The distribution of the $\delta^{13}C$ values over the stratigraphic series can be seen in Figure 3, plotted with the corresponding stratigraphic sections linked to each sample run for $\delta^{13}C$. The overall average trend of $\delta^{13}C$ values is -0.1525x – 1.2448, showing that as the samples get younger, the values become lower on average. There are four major negative excursions with samples TC-07-05, SH-07-04, IS-07-04, and MD-19-08, with MD-19-08 being the lowest, at a

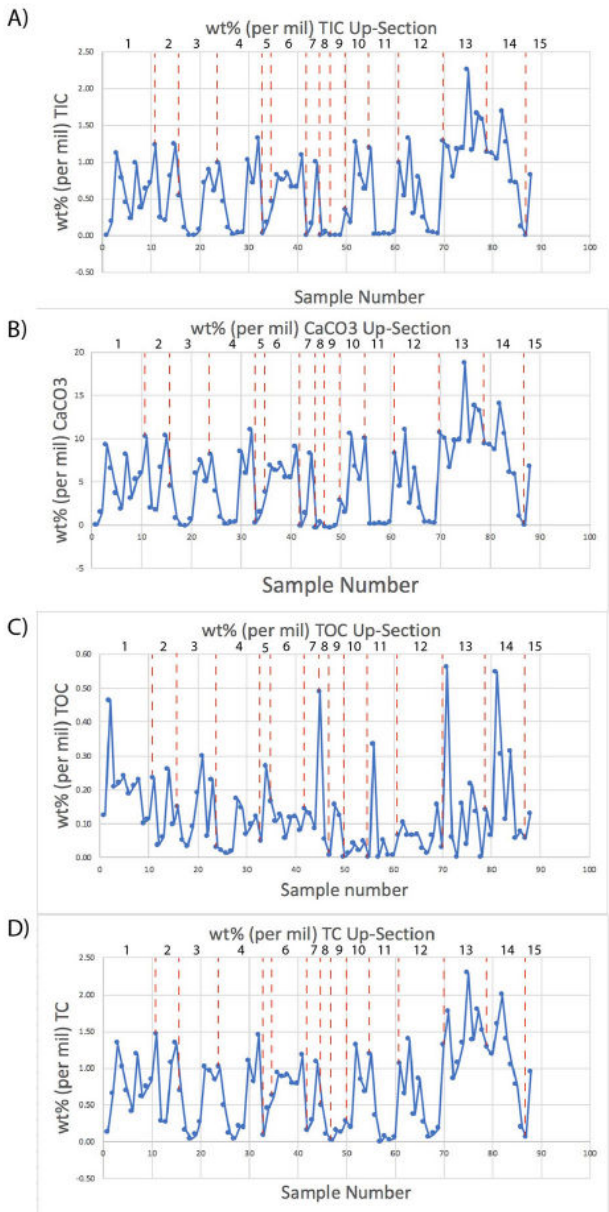

Figure 4. Total Inorganic Carbon (TIC), Calcium Carbonate (CaCO3), and Total Organic Carbon (TOC) and Total Carbon (TC) for each site with A) wgt. % TIC; B) wgt. % CaCO3; C) wgt. % TOC, and D) wgt. % TC. Numbers at top of each plot correspond to a stratigraphic section from the field, defined by the red-dashed margin: 1 = TC-01, 2 = MD-02, 3 = MD-09, 4) = SH-07, 5 = MF-08, 6 = KS-04, 7 = KS-01, 8 = MD-04, 9 = RG-03, 10 = SH-01, 11 = MF-07, 12 = ER-04, 13 = MD-19, 14 = IS-07, 15 = MF-05.

$\delta^{13}C$ value of -7.9‰. As all the samples from the whole dataset could not be run due to their low $CaCO_3$ content, the only complete stratigraphic section that could be analyzed was the MD-19 section. This interval shows a high degree of variability in terms $\delta^{13}C$ values, and the trend is negative up-section. The highest value in the section is -1.1‰ $\delta^{13}C$ and the lowest value is -7.9‰ $\delta^{13}C$.

DISCUSSION

The goal of this project is to provide a chronostratigraphic framework for the fossil samples collected from the Fort Union and Willwood Formations. As seen in Figure 3, the trend in $\delta^{13}C$ becomes lower further up-section, suggesting a significant negative excursion part-way through the MD-19 section. This shift towards lower values is similar to that shown by $\delta^{13}C_{carb}$ analysis done by Baczynski et al. (2013) and Koch et al. (2003), coinciding with the overall transition between the Fort Union Formation and the Willwood Formation. Since sampled sections begin in the Fort Union Fm., down-section of where the PETM $\delta^{13}C$ excursion and Fort Union-Willwood contact occurs, I interpret the negative shift to mark the transition between the two formations, agreeing with the studies of Baczynski et al. (2013) and Koch et al. (2003). The PETM appears to occur in section MD-19 when the isotopic record trends to the most negative values among the collected samples.

There is a marked difference between the $\delta^{13}C$ values presented by Baczynski et al. (2013) and those measured in this study. Their values average between -14 to -16‰ $\delta^{13}C_{carb}$ whereas the most negative value for the bulk $\delta^{13}C_{carb}$ recorded here is -7.9‰, indicating that there may have been multiple sources of carbonate present in the bulk samples. Baczynski et al. (2013) drilled samples from carbonate nodules using a Dremel tool on a polished section face in order to avoid secondary diagenetic spar. Thus, the very light $\delta^{13}C$ values measured in their study reflect authigenic carbonate. Since there were not enough carbonate nodules distributed through the sampled section used in this study to allow a continuous series for isotopic analysis, bulk sample was the only option. The bulk samples likely include carbonate phases with more isotopically enriched carbon. Further analysis of this difference and subsequent interpretations can be pursued after collection of $\delta^{13}C$org data.

CONCLUSION

Upon examination of the stable isotope data, the $\delta^{13}C$ values presented through the geochemical analysis of Paleogene-age sediments for the Bighorn Basin show

the negative $\delta^{13}C$ excursion near the PETM and Fort Union-Willwood Formational contact. These results suggest that the PETM occurs within section MD-19. This suggests that if dwarfism occurs in *Coryphodon* in association with PETM climate changes, it should manifest in specimens from sections MD-19 and IS-07. The geochemical data described herein help constrain the chronology of the collected *Coryphodon* samples, thus contributing to the study of effects of Paleogene hyperthermals on dwarfism within mammalian fauna. This work will provide further evidence on the physical and morphological effects that a warming climate may have on mammals. Analogous to the PETM, anthropogenic activities over the past century are driving a rapid increase in of atmospheric CO_2 levels and a significant rise in global temperature. Continued study of the PETM will surely contribute to growing understanding of the effects of rapid warming on mammalian taxa.

ACKNOWLEDGMENTS

This research is financially supported by the Keck Geology Consortium and the National Science Foundation under Grant No.1659322, as well as Northwestern Weinberg College of Arts and Sciences Summer Research Grant. Thanks to my research advisors, Michael D'Emic, Simone Hoffmann, Brady Foreman, and Matthew Hurtgen, as well as fellow Keck researchers, Emily Randall, Danika Mayback, Grant Bowers, Richard Gonzalez, and Michael Ford, and my lab managers Grace Schellinger and Andrew Masterson.

REFERENCES

Abels, H.A., Clyde, W.C., Gingerich, P.D., Hilgen, F.J., Fricke, H.C., Bowen, G.J., and Lourens, L.J. (2012) Terrestrial carbon isotope excursions and biotic change during Palaeogene hyperthermals. Nature Geoscience, 5, 326–329.

Baczynski, A. A., Mcinerney, F. A., Wing, S. L., Kraus, M. J. (2013) Chemostratigraphic Implications of spatial variation in the Paleocene-Eocene Thermal Maximum carbon isotope excursion, SE Bighorn Basin, Wyoming. Geochemistry. Geophysics. Geosystems, 14, 4133–4152.

Barnosky, A.D., Hadly, E.A., Gonzalez, P., Head, J., Polly, P.D., Lawing, A.M. et al. (2017) Merging paleobiology with conservation biology to guide the future of terrestrial ecosystems. Science, 355, eaah4787.

D'Ambrosia, A.R., Clyde, W.C., Fricke, P.D. Gingerich, and Abels, H.A. (2017) Repetitive mammalian dwarfing during ancient greenhouse warming events. Science Advances, 3, e1601430.

Engleman, E. E., Jackson, L. L., and Norton, D. R. (1985) Determination of carbonate carbon in geological materials by coulometric titration. Chemical Geology, 53, 125–128.

Gingerich, P.D. (2003) Mammalian responses to climate change at the Paleocene-Eocene boundary: Polecat Bench record in the northern Bighorn Basin, Wyoming. Geological Society of America Special Paper, 369, 463–478.

Koch, P. L., Clyde, W. C., Hepple, R. P., Fogel, M. L., Wing, S. L., Zachos, J. C. (2003) Carbon and oxygen isotope records from Paleosols spanning the Paleocene-Eocene boundary, Bighorn Basin, Wyoming. Geological Society of America Special Papers, 369, 49–64.

Palkovacs, E.P. (2003) Explaining adaptive shifts in body size on islands: A life history approach. Oikos, 103, 37–44.

Secord, R., Bloch, J.I., Chester, S.G.B., Boyer, D.M., Wood, A.R., Wing, S.L., Kraus, M.J.,McInerney, F.A., and Krigbaum, J. (2012) Evolution of the earliest horses driven by climate change in the Paleocene-Eocene Thermal Maximum. Science, 335, 959–962.

Zachos, J.C., Dickens, G.R., and Zeebe, R.E. (2008) An early Cenozoic perspective on greenhouse warming and carbon-cycle dynamics. Nature, 451, 279–283.